Fabrication of Bioinspired Actuated Nanostructures with Arbitrary Geometry and Stiffness

Submitted to ADVANCED MATERIALS

DOI: 10.1002/adma.((please add manuscript number))

Fabrication of Bio-Inspired Actuated Nanostructures with Arbitrary Geometry and Stiffness**

By *Boaz Pokroy, Alexander K Epstein, Maria C. M. Gulda Person,* and *Joanna Aizenberg**

[*] Prof. Dr. J. Aizenberg, Dr. B. Pokroy, Mr. A.K Epstein, Ms. M.C.M. Gulda Person
School of Engineering and Applied Sciences, Harvard University
29 Oxford Street, Cambridge, MA 02138 (USA)
E-mail: (jaiz@seas.harvard.edu)

Prof. J. Aizenberg
Department of Chemistry and Chemical Biology, Harvard University
12 Oxford Street, Cambridge, MA 02138 (USA)

[**] We would like to thank Prof. J. J. Vlassak and H. Li for the use of the 4-point flexure apparatus and Prof. G. M. Whitesides and Dr. M. Reches for access to their equipment during the construction of J.A.'s lab. We thank Dr. A. Taylor for the fabrication of Si nanostructures. B.P. would like to extend his gratitude to the Fulbright Visiting Scholar Program for financial support. This work was partially supported by the Materials Research Science and Engineering Center (MRSEC) of the National Science Foundation under NSF Award Number DMR-0213805.

Keywords: ((Five maximum))

Biology is replete with examples of functional structures, whose properties are unmatched in today's man-made materials. Key features of biological structures are their dynamic nature, responsive behavior and often multi-functionality, which all comprise the goals for the next-generation smart artificial materials. There is a growing body of information describing natural structures with sophisticated design strategies that lend the organisms and plants superior mechanical, optical, adhesive, self-cleaning, actuation and sensing capabilities.[1–9] Interestingly, the common feature of these largely unrelated designs is the use of fibers and high-aspect-ratio nano- and micro-structures. Nanostructures on the surface of the lotus leaf make the leaves superhydrophobic, and the droplets of water containing the collected insects and dust will roll off, and so maintain a clean leaf surface.[1] A gecko's feet are comprised of half a million setae fibers. Each seta is tipped with ~1000 nanometer-sized spatulae. This multi-scale fibrous assembly offers a unique, reversible

adhesion mechanism that holds geckos to surfaces in a self-cleaning fashion.[2,3] Complex, hierarchically-structured high-aspect-ratio silica fibers in the sponge Venus's Flower Basket provide amazing fiber-optical capabilities combined with superior mechanical properties.[4,5] Fish and amphibians have fibrous structures (cilia) on the surfaces of their bodies connected to a hair cell at their base that detect water flow.[6,7] Due to this sensing ability fish can swim in narrow caves—even without the possibility for eye sight—and sense other organisms moving in their vicinity.[6] Echinoderms cover their skin with high-aspect-ratio spines and mobile pedicellaria that provide an effective antifouling mechanism, preventing the settlement and growth of other organisms, by active movement.[8] Pedicellaria—small claw-like extensions on the aboral surface of starfish and sea urchins—essentially exist as dense arrays of environmentally responsive biological μ-actuators.[8]

It has been a long-standing aspiration of bio-inspired materials science to understand the underlying construction principles of biological materials and to reproduce their unique features synthetically. We asked ourselves the question whether it is feasible to design a finely tunable, multifunctional, responsive nanostructured material that will show self-cleaning properties à la lotus leaf, will be capable of movement and reversible actuation à la echinoderm spines and pedicellaria and of sensing the force field à la fish skin. While nanostructured superhydrophobic surfaces inspired by the lotus flower and the adhesive properties of gecko feet have been mimicked with success,[10–12] actuation/sensing at the sub-micron scale is a challenging goal. Sensor arrays inspired by fish skin[13] are still lacking the key features related to their selectivity, tunable geometry and sensitivity. We have recently demonstrated that by using a hydrogel muscle one can reversibly actuate Si nanostructures, which dynamically change their orientation in response to humidity, with a 60 ms response time.[14] While providing a successful example of a bio-inspired approach to controlled actuation at the nanoscale, this hybrid design had several structural limitations, including: (i) the nanostructures themselves were passive units and their movement was induced by a

hydrogel that responded to one stimulus; (ii) the nanostructures were made of Si and, therefore, they had a fixed, high degree of stiffness that restricted the deflection and required high forces; and (iii) with no control over the stiffness, the extent of actuation was adjusted by using Si nanoarrays with various aspect ratios, which involved a highly expensive and labor-intensive deep-etching fabrication procedure for each substrate. In the current study we wanted to take this bio-inspired design to the next level and use a truly "*materials*" approach to develop a low-cost procedure for producing an arbitrarily-designed actuated surface with high-aspect-ratio nanostructures that are themselves responsive to a variety of stimuli and have a finely-tuned geometry and stiffness.

Fabrication procedure. A soft lithography technique has been introduced recently as a low-cost alternative to the conventional lithography and has been shown to be an extremely powerful method for the high-resolution replication of microfabricated substrates in an elastomeric polymer – polydimethylsiloxane (PDMS).[15–17] PDMS has been widely used to form polymeric arrays of micron-sized posts for a variety of applications, including control of cellular adhesion and wettability.[18–20] Due to the low level of stiffness of PDMS, only limited aspect ratios were achievable, and irreversible collapse was shown to occur in high-aspect-ratio posts.[21] We have adopted and significantly extended the soft lithography replication method, to allow the fabrication of a biomimetic array of stable, high-aspect-ratio features, which represents a critical functional requirement of biological actuated nanostructures and sensors. In our approach, PDMS is not the final nanostructured material: it is used as a secondary elastomeric mold for casting the replica in the material of choice. As a result, the stability and stiffness of the replicated structures can be controlled by choosing as the final material one with the desired mechanical properties, and the geometry of the nanostructures can be finely-tuned by applying a specific deformation of the PDMS mold.

The fabrication procedure is outlined in **Figure 1**. The initial high-aspect-ratio master can be either formed by standard lithographical techniques, grown bottom-up (for example,

nanowires) or a biological sample. In this paper, we demonstrate our procedure by replicating arrays of Si nanoposts with the pitch a_0 (distance between the posts), the post radius r_0 and length l_0 (Fig. 1A). We formed a negative replica of the structure coated with an anti-sticking thin layer in PDMS or paraffin (Fig. 1B-E). An important requirement is that the negative replica must be able to peel off or detach easily without disrupting the Si fine structure, so that the features are accurately replicated on a large scale (Fig. 1C). The created PDMS or paraffin mold (Fig. 1D-E) has an array of wells, into which the desired material (polymer, liquid metal or ceramics) is cast in liquid form and cured (Fig. 1F). The mold is then either peeled off (PDMS) (Fig. 1G) or heated and dissolved (paraffin) to reveal the replicated structure. Figure 1H shows an epoxy-replicated nanoarray that reproduces the original master with the nanometer-scale resolution. These surfaces exhibit superhydrophobic, self-cleaning properties and the water droplets remain suspended on the tips of the nanoarray and roll off the surface, similar to the properties reported for the original Si masters.[22,23]

Controlling the geometry of nanostructures. The fabrication of nanostructures with different geometries using this one-to-one double-replication procedure would require specialized, highly expensive Si masters for each design. Moreover, the lithographic procedure allows only the generation of nanostructures oriented normal to the surface. In the case of our biological "role models," the high-aspect-ratio fibers are often oriented in different directions, rather than just standing upright,[8] and have non-circular cross-sections.[7] This asymmetry has important functional implications. For example, it can lead to anisotropy in the adhesive properties[24] of gecko feet on surfaces or to anisotropy in wettability in some man-made nanostructured surfaces.[25] The elliptical cross-section of superficial neuromasts—structures that detect water flow on the body surface of fish and amphibians—provides the ability to map the direction of water flow.[13] Motivated by these considerations we have developed a technique, by which we can easily control the geometry of the nanostructures to form both tilted and twisted posts, as well as different 2D symmetries and cross-sectional

shapes, using the same original master. This is achieved by deforming the flexible negative PDMS molds before curing or solidifying the final material.

Certain exemplary deformation types are shown in **Fig. 2** and the resulting changes in geometry are summarized in **Table 1**. By deforming the PDMS negative molds via stretching or compression in the principal directions of the 2D array of posts, we can transform the original 2D square lattice to a rectangular or rhombic lattice and the original circular cross-sections of the nanoposts to elliptical (Table 1, Fig. 2A-C). By deforming the mold in the general [*hk*0] direction, a parallelogram unit cell with finely-tuned parameters can be formed. The amount of the deformation determines both the degree of ellipticity and the unit cell of the nanoarray. Tilted structures can be formed by applying a shear deformation to the mold. The amount of the shear determines the tilt angle, and the direction of the shear determines the tilt direction. The length of the posts, l_0, can be changed by compressing the negative mold perpendicular to the 2D array (Table 1, Fig. 2F). We also have the ability to form twisted nanostructures (Fig. 2E) or curved surfaces with different radii of curvature (concave or convex) very similar to echinoderm skin (Fig. 2D,H). To ensure the fabrication of an arbitrary array of nanostructures, any combination of the deformation types can be applied. **Figure 3** shows an example of an epoxy nanostructured surface that was fabricated using a compound deformation of the mold consisting of a square array of normally-oriented, 8 μm-deep, circular wells with a_0 = 2 μm and r_0 = 125 nm. By applying a 20% stretch and 12.5% shear in the [110] direction, we created a structure that exhibits tilted nanoposts with $t \cong 7°$, $\theta \cong 78°$ and $a \cong 2.18$ μm.

When engineering a functional surface bearing high-aspect-ratio nanoposts, one should consider the stability of the expected structures. There are several factors that can lead to the collapse of nanoposts[26]: a collapse due to the self-weight[27]; adhesion forces between the posts and the base surface[21]; and lateral adhesion.[27] Calculations show that the first two are much too small to affect our structures; however, the importance of the second factor

increases with the fabrication of the tilted nanostructures. The lateral adhesion force is the strongest of the three and has to be taken into account. The critical aspect ratio, below which there will be no lateral collapse, is given by[21, 26]

$$\frac{l}{d} = \left(\frac{0.57 E^{1/3} a^{1/2}}{\gamma_s^{1/3} d^{1/6} (1-\nu^2)^{1/12}} \right) \quad (1)$$

where d is the diameter of the posts, γ_s is the surface energy and ν is the Poisson ratio of the nanostructured material and a is the pitch.

Controlling the stiffness. An additional advantage of using the soft lithography procedure to replicate the original master is the ability to regulate the stiffness of the resulting nanostructures. For example, the stiffness of the nanostructured array with the same geometry can vary from a few MPa to hundreds of GPa when the replicas are made out of polymers and metals/ceramics, respectively. Even more importantly, the stiffness of the array can be finely tuned by mixing in different proportions two polymers that show high and low stiffness. To demonstrate this capability, we have chosen to use two epoxy-based polymers: a high-viscosity resin with a post-cure higher modulus, and a low viscosity resin with a post-cure low modulus. We were able to produce epoxy structures with a stiffness that ranges from a MPa to several GPa, a range of four orders of magnitude (**Fig. 4**). Figure 4 can be then used as a calibration curve to define the recipe for a polymer mixture that will endow a nanopost array with an arbitrary, required stiffness in the MPa-GPa range. This latter point is extremely important as regards the fine-tuning of the sensing/actuation capability of the nanostructures.

Actuation of the nanostructures. The mechanics of the movement of the posts is a key issue when designing functional nanostructured materials for applications in actuation/sensing. We have previously shown that when a force is applied on the beam parallel to the initial direction of the un-bent post, there is a critical force below which no bending (buckling) occurs.[14] When the force F acts along the entire post length, l, perpendicular to the posts, the deflection, Y_{lz}, at a given point l_z from the base is given by[28] $Y_{l_z} = F l_z^{\,3} / 8EI$, where E is the

bending modulus and I is the moment of inertia. For a post with a circular cross-section with the radius r, the moment of inertia is given by the relation $I = \pi r^4/4$. To obtain an estimate for the forces needed to actuate the structures we are producing, we can use some feasible characteristic values: E = 1 GPa, l = 8 μm, r = 125 nm. In this case, to deflect the tip of the post by 0.5 μm, one would need a force of about 1.5 nN. If the same force F is applied only to the tip of the post, the tip will deflect 2.67 times more ($Y_{l_z} = Fl_z^3 / 3EI$).

A bio-inspired example of the application of these nanoarrays is in flow sensors. If the structures are chemically treated to be superhydrophobic, only the tips of the posts will sense the flow. However if alternatively the whole structure is hydrophilic, then the force of the flow will act on the entire post. Moreover, the demonstrated unique capability of our approach to create nanostructures with elliptical cross-sections makes it possible to design a truly biomimetic sensor that responds to an anisotropic flow field in a manner, similar to cilia in fish and amphibians.[13] In this case, the moment of inertia in the directions of the two radii will be: $I_1 = \pi r_1^3 r_2/4$ and $I_2 = \pi r_1 r_2^3/4$, and for the given force, the deflection in the direction of r_1 compared to r_2 scales as $(r_2/r_1)^2$.

To increase the sensitivity of the nanoarray, we can reduce the radius (which scales as a power of four), increase the length (scales as a power of three), and decrease the modulus (linear dependence). Graphs that demonstrates the force needed to bend the posts as a function of different parameters is shown in **Fig. 5**. As different geometrical and mechanical parameters all have an effect on the force needed to actuate the posts, it is very helpful to introduce a unified "effective stiffness" parameter, S_{effect}, to compare the different cases. We chose to define this parameter as the force per unit deflection of the posts: $S_{effect} = F / Y_{l_z}$. In order to compare two structures, we take the ratio of the two S_{effect}. For a circular cross-section:

$$\frac{S_{1effect}}{S_{2effect}} = \left(\frac{E_1}{E_2}\right)\left(\frac{l_2}{l_1}\right)^3\left(\frac{r_1}{r_2}\right)^4 \quad (2)$$

This dimensionless parameter allows the direct and simple comparison of the actuation capabilities of the nanostructures.

Due to the relatively low forces needed to move the posts in our typical structures, we can observe the actuation under the Scanning Electron Microscope (SEM) (see **Fig. 6**A-B**)** and Movie 1 in the supporting online information). In this case, the actuation is probably driven by the electrostatic forces imposed by the e-beam.[29] This movement is reversible and can be repeated multiple times: the posts bend into the e-beam when the beam is focused on a small area, and return to their normal orientation once the e-beam is not concentrated on a small scanning area. The actuation of the array of tilted nanoposts (as in many biological systems) is shown in Fig. 6C and Movie 2 in the supporting online information. We emphasize that this is only an illustration of the ability of these posts to respond in a controlled manner to an external force.

We are currently developing bio-inspired nanostructures that actuate in response to a variety of stimuli, such as magnetic, acoustic, piezoelectric, and chemical. It is noteworthy that previous efforts in actuation/sensing on the nanometer scale have used unorganized 2D arrays of high-aspect-ratio nanostructures (see for example Ref. [30]). Our biological role models are often comprised of ordered arrays of spicules, ciliated cells or pedicellaria. The ordered 2D arrays of high-aspect-ratio nanostructures described here have the advantage of providing homogeneous, traceable parameters over large length scales, from a sub-micron scale to a centimeter scale.

In conclusion, we have shown that we can produce versatile high-aspect-ratio nanostructured surfaces inspired by the echinoderm skin, gecko foot and superficial neuromasts in fish and amphibians. For this purpose, we have developed a soft-lithographic method that not only allows the one-to-one replication of nanostructures with high-aspect-

ratios in a variety of materials, but also makes it possible to produce arbitrary nanostructures with cross-sectional shapes, orientations, and 2D lattices that are different from the original master. This method is the only one to our knowledge that provides such a high degree of tunability of mechanical parameters at the nanoscale and the formation of nontrivial geometries, including tilted or twisted nanostructures. The resulting bio-inspired surfaces offer multifunctional characteristics that include superhydrophobic character, actuation and sensing capabilities. We believe that these structures will find exciting applications as "smart" sensors, actuators and other dynamic materials.

Experimental

An array of silicon nanoposts was fabricated using the Bosch process, as described elsewhere.[22,31] The silicon nanopost arrays were treated with an anti-sticking agent (tridecafluoro-1,1,2,2-tetrahydrooctyl)-trichlorosilane (Gelest Inc.) by exposure in a desiccator under vacuum overnight.

Negative replicas were produced from polydimethylsiloxane (PDMS) (Dow-Sylgard 184) with a prepolymer-to-curing agent ratio of 10:1. After extensive mixing of the prepolymer and curing agent, the mixture was poured on the silicon nanopost substrate and placed in a vacuum desiccator for one hour to eliminate all air bubbles. It was then thermally cured in an oven for 3 hours at 70° C. After cooling, the negative PDMS mold was gently peeled off the substrate. The negative PDMS mold was then cleaned extensively with ethanol, isopropanol, and acetone sequentially, dried and treated in nitrogen plasma for 1 min in a Femto Diener® plasma cleaner. After this surface treatment, the negative mold was placed in (tridecafluoro-1,1,2,2-tetrahydrooctyl)-trichlorosilane environment in a desiccator under vacuum overnight.

In order to produce the final replica of the master one pours the desired material in liquid form into the negative replica wells (Fig. 1F). It is essential to ensure that this material

completely fills the negative replica and solidifies inside it. In order to prevent the formation of bubbles trapped between the mold material and the original structure, a vacuum is applied over the liquid. Once the material has solidified, the negative replica is simply peeled off, leaving behind the free-standing nanostructured material. Using this method one can form replicated nanostructures from a variety of materials such as: polymers (e.g. epoxy, PP, PE, PVA, PMMA, PDMS, various hydrogel and shape memory polymers) and metals and alloys which have a low melting point (e.g. Ga, InBi and Woods alloy). In this study most of the nanostructured replicas were made from a commercial UV-initiated one-part epoxy UVO-114^{TM} (Epoxy Technology). This epoxy was chosen due to the ease of use and a relatively high bending stiffness of about 1 GPa.

For the experiments involving the control of the flexural modulus of the nanostructures, two liquid epoxy resins—Dow D.E.R. 331™, a liquid reaction product of epichlorohydrin and bisphenol A, and Dow D.E.R. 732™, a viscosity-reducing reaction product of epichlorohydrin and polypropylene glycol—were mixed in different proportions. The mixtures were based on 10% increments of components by weight, from 10 % to 100 %. In all compositions, UV cross-linking initiator Cyracure UVI 6976™ (Dow) was added to the mixture in a constant 5 weight % amount.

To produce 4-point flexure test epoxy samples, 10x8x62 mm custom aluminum blocks were placed in a glass bowl; PDMS was poured and cured as described above to create molds. Each of the eleven epoxy mixtures as well as the commercial UV-initiated one-part epoxy UVO-114^{TM} (Epoxy Technology) were sequentially pipetted into the PDMS molds flush with the tops of the wells. Each flexure sample was cured by placing molds directly under a B-100 ultraviolet lamp (UVP Blak-Ray) inside a photochemical cabinet until fully cured, which required from 20 minutes to several hours depending on the composition. Mixtures with higher percentage of D.E.R. 331 required more time to crosslink.

A custom-built mechanical test system was used to test the epoxy samples in 4-point bending and determine their flexural modulus. The system had a displacement resolution of 10 nm, controlled by a precise step motor with 100 N capacity, and a load resolution of 0.01 N. It was set up on a pneumatic table to shield against vibration and was operated by a PC through LabView. The fixture's upper anvil pins were set at 28 mm apart and lower pins were spaced at 56 mm. A displacement rate of 500 μm/s and a maximum deflection of 3 mm was used for compliant samples, decreasing to 0.5-1.5 mm deflection for stiffer samples, as dictated by the step motor maximum load. The load-deflection data were plotted into linear elastic curves whose slopes were calculated and, along with the anvil and sample geometries, were used in the 4-point bending equation to obtain the flexural moduli of the epoxy replicas.

Imaging of the nanostructures was done by a Zeiss field emission Ultra55 SEM. Chemical analysis was carried out on the SEM using Energy Dispersive Spectroscopy (EDS).

Received: ((will be filled in by the editorial staff))
Revised: ((will be filled in by the editorial staff))
Published online: ((will be filled in by the editorial staff))

References

_[1] W. Barthlott, C. Neinhuis, *Planta* **1997**, *202*, 1–8.

_[2] R. Ruibal, V. Ernst, *J. Morphol* **1965**, *117*, 271–293.

_[3] K. Autumn, S. T. Hsieh, D. M. Dudek, J. Chen, C. Chitaphan, R. J. Full, *J. Exp. Biol.* **2006**, *209*, 260–272.

_[4] J. Aizenberg, V. C. Sundar, A. D. Yablon, J. C. Weaver, G. Chen, *Proc. Natl. Acad. Sci. U. S. A.* **2004**, *101*, 3358–3363.

_[5] V. C. Sundar, A. D. Yablon, J. L. Grazul, M. Ilan, J. Aizenberg, *Nature* **2003**, *424*, 899–900.

_[6] M. J. McHenry, S. M. van Netten, *J. Exp. Biol.* **2007**, *210*, 4244–4253.

_[7] J. Montgomery, S. Coombs, *Brain Behav. Evol.* **1992**, *40*, 209–216.

_[8] E. E. Ruppert, R. S. Fox, R. B. Barnes, *Invertebrate Zoology*, Brooks Cole Thomson, Belmont, CA **2004**.

_[9] G. Huber, H. Mantz, R. Spolenak, K. Mecke, K. Jacobs, S. N. Gorb, E. Arzt, *Proc. Natl. Acad. Sci..U. S. A.* **2005**, *102*, 16293–16296.

[10] P. F. Rios, H. Dodiuk, S. Kenig, S. McCarthy, A. Dotan, *J. Adhes. Sci. Technol.* **2007**, *21*, 399–408.

[11] A. K. Geim, S. V. Dubonos, I. V. Grigorieva, K. S. Novoselov, A. A. Zhukov, S. Y. Shapoval, *Nat. Mater.* **2003**, *2*, 461–463.

[12] A. del Campo, C. Greiner, E. Arzt, *Langmuir* **2007**, *23*, 10235–10243.

[13] S. Peleshanko, M. D. Julian, M. Ornatska, M. E. McConney, M. C. LeMieux, N. Chen, C. Tucker, Y. Yang, C. Liu, J. A. C. Humphrey, V. V. Tsukruk, *Adv. Mater.* **2007**, *19*, 2903–2909.

[14] A. Sidorenko, T. Krupenkin, A. Taylor, P. Fratzl, J. Aizenberg, *Science* **2007**, *315*, 487–490.

[15] Y. N. Xia, G. M. Whitesides, *Ann. Rev. Mater. Sci.* **1998**, *28*, 153–184.

[16] Y. N. Xia, G. M. Whitesides, *Angew. Chem., Int. Ed.* **1998**, *37*, 551–575.

[17] Y. N. Xia and G. M. Whitesides, *Angew. Chem., Int. Ed.* **1998**, *37*, 551-575.

[18] J. L. Tan, J. Tien, D. M. Pirone, D. S. Gray, K. Bhadriraju, C. S. Chen, *Proc. Natl. Acad. Sci. U. S. A.* **2003**, *100*, 1484–1489.

[19] Z. J. Zheng, O. Azzaroni, F. Zhou, W. T. S. Huck, *J. Am. Chem. Soc.* **2006**, *128*, 7730–7731.

[20] L. Courbin, E. Denieul, E. Dressaire, M. Roper, A. Ajdari, H. A. Stone, *Nat. Mater.* **2007**, *6*, 661–664.

[21] P. Roca-Cusachs, F. Rico, E. Martinez, J. Toset, R. Farre, D. Navajas, *Langmuir* **2005**, *21*, 5542–5548.

[22] T. N. Krupenkin, J. A. Taylor, T. M. Schneider, S. Yang, *Langmuir* **2004**, *20*, 3824–3827.

[23]A. Ahuja, J. A. Taylor, V. Lifton, A. A. Sidorenko, T. R. Salamon, E. J. Lobaton, P. Kolodner, T. N. Krupenkin, *Langmuir* **2008**, *24*, 9–14.

[24] B. X. Zhao, N. Pesika, K. Rosenberg, Y. Tian, H. B. Zeng, P. McGuiggan, K. Autumn, J. Israelachvili, *Langmuir* **2008**, *24*, 1517–1524.

[25]A. D. Sommers, A. M. Jacobi, *J. Micromech. Microeng.* **2006**, *16*, 1571–1578.

[26] Y. Zhang, C. W. Lo, J. A. Taylor, S. Yang, *Langmuir* **2006**, *22*, 8595–8601.

[27] C. Y. Hui, A. Jagota, Y. Y. Lin, E. J. Kramer, *Langmuir* **2002**, *18*, 1394–1407.

[28] A. R. Ragab, S. E. A. Bayoumi, *Engineering Solid Mechanics: Fundamentals and Applications*, CRC Press, Boca Raton, FL **1998**, p. 944.

[29] The mechanism of the actuation under e-beam will be reported elsewhere.

[30] B. A. Evans, A. R. Shields, R. L. Carroll, S. Washburn, M. R. Falvo, R. Superfine, *Nano Lett.* **2007**, *7*, 1428–1434.

[31] S. A. McAuley, H. Ashraf, L. Atabo, A. Chambers, S. Hall, J. Hopkins, G. Nicholls, *J. Phys. D: Appl. Phys.* **2001**, *34*, 2769–2774.

[32] J. C. Lotters, W. Olthuis, P. H. Veltink, P. Bergveld, *J. Micromech. Microeng.* **1997**, *7*, 145–147.

Figure 1. Two-step soft lithography process for creating replicas of nanostructured surfaces with high-aspect-ratio features. A) SEM image of an exemplary original nanostructured surface—a silicon master bearing a square array of 8-µm-long posts with the diameter of 250 nm and the pitch of 2 µm. The oblique view is used to best visualize the structure. The insert is an EDS spectrum. B) Liquid PDMS precursor is poured onto the master treated with an anti-sticking agent and cured. C) The cured PDMS is peeled off from the master. D) The negative PDMS mold, which contains an array of high-aspect-ratio wells corresponding to the posts of the positive master, is surface-treated with an anti-sticking agent. E) SEM image of the PDMS mold, revealing the high-aspect-ratio wells. F) Liquid precursor (polymer, liquid metal) is poured onto the negative PDMS mold and cured. G) The PDMS mold is peeled from the cured positive replica. H) SEM image of an exemplary nanostructured replica fabricated from epoxy resin. The insert is an EDS spectrum. The replicated structure is geometrically indistinguishable from the master shown in A).

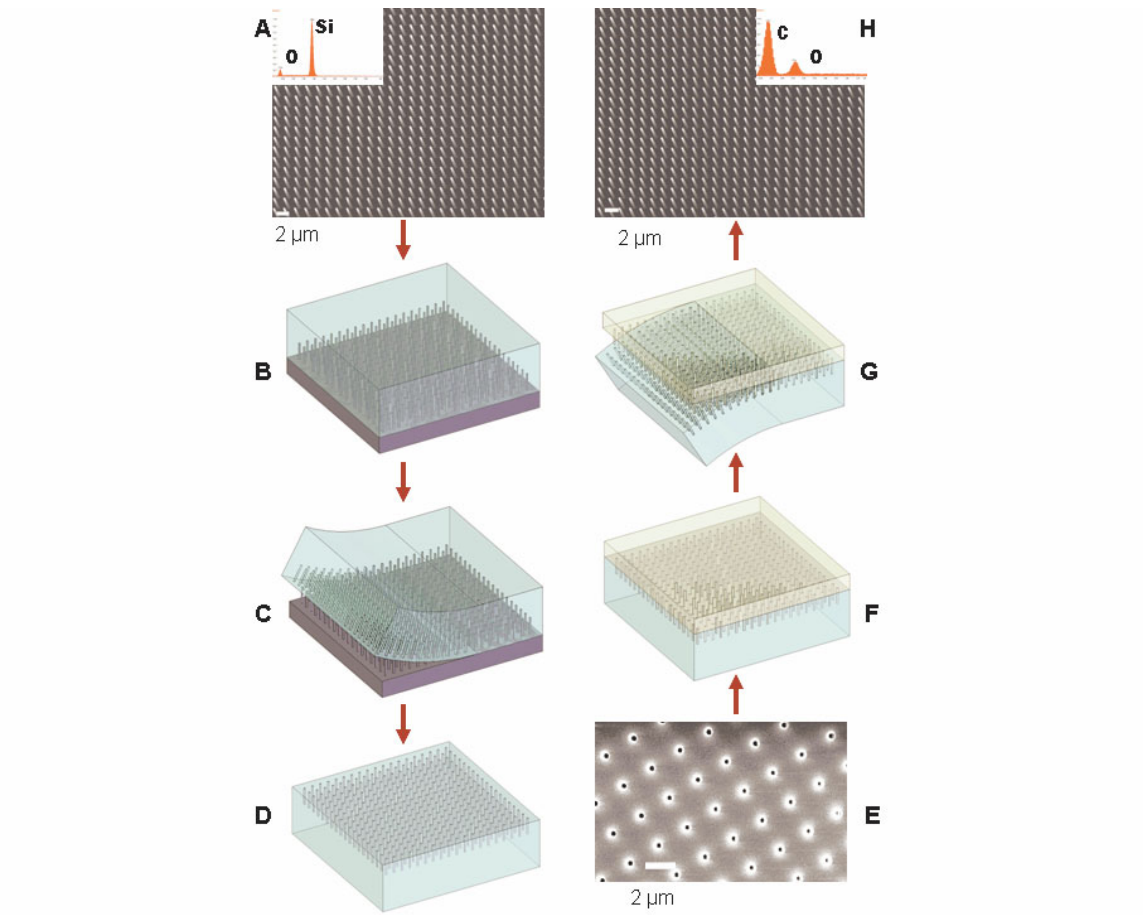

Figure 2. Schematic three-dimensional renderings of various deformations of the PDMS mold, which allow the fabrication of arbitrary arrays of nanoposts with finely-tuned geometries and nontrivial configurations. The unmodified mold (center) can be: A) compressed along the [100] direction; B) stretched along the [100] direction; C) stretched along the [110] direction; D) uniformly curved concavely; E) torsioned around the [001] axis; F) compressed along the [001] direction; G) sheared along the [100] direction; or F) uniformly curved convexly.

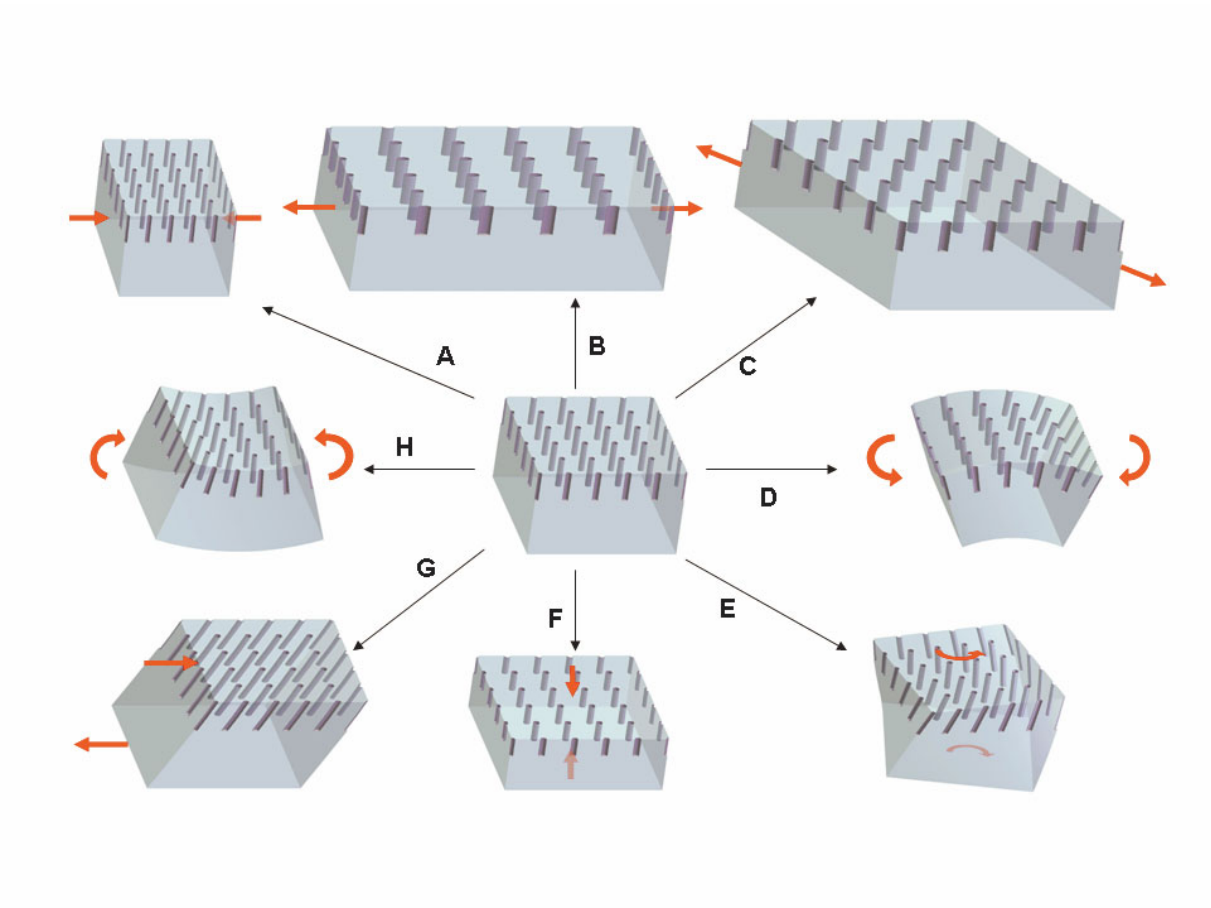

Figure 3. SEM image of an epoxy nanopost array fabricated using a compound deformation that included a 20% stretch and 12.5% shear in the [110] direction, viewed normal to the surface. The 2D array of posts displays a rhombic symmetry (unit cell highlighted in red). This combined deformation-mode created a structure that exhibits tilted nanoposts with $t \cong 7°$, $\theta \cong 78°$ and $a \cong 2.18$ μm.

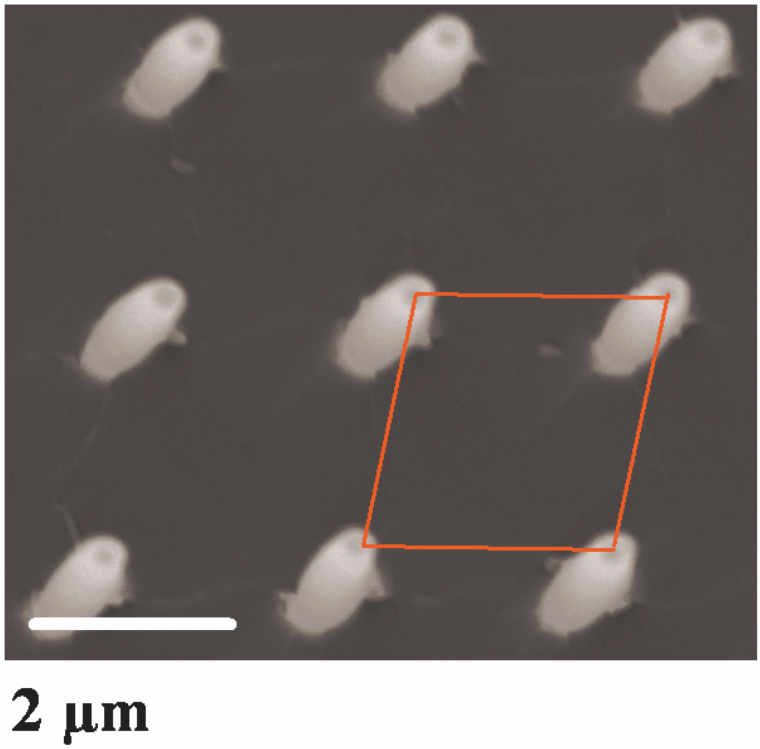

Figure 4. Histogram presenting four orders of magnitude in post flexural modulus as a function of the ratio of D.E.R. 331 (stiff epoxy resin) to D.E.R. 732 (soft epoxy resin) in weight percent. The tests were performed on a 4-point flexure tester and thus reflect pure bending conditions.

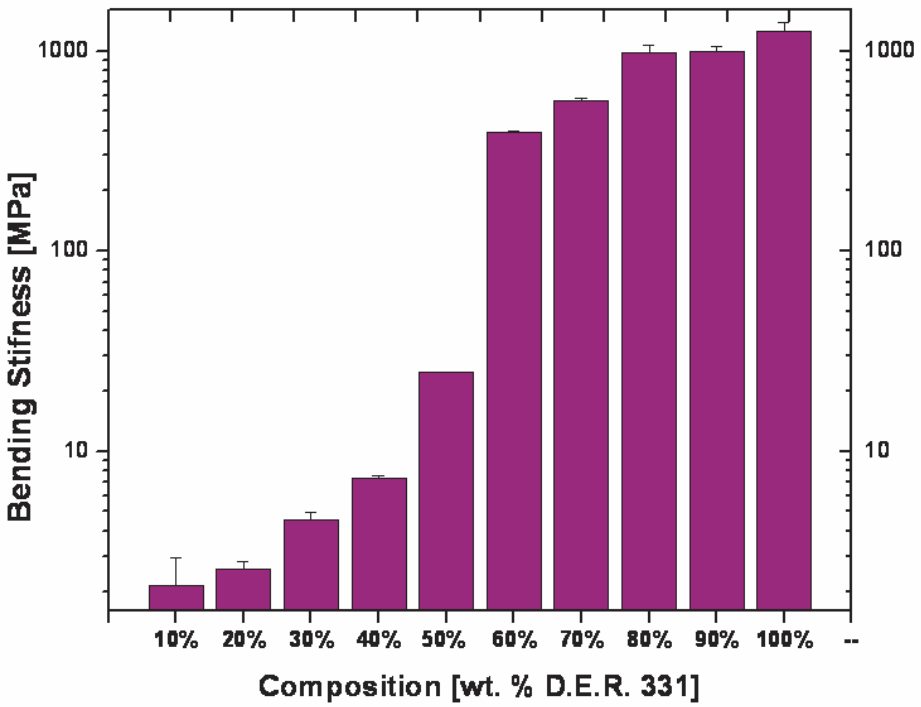

Figure 5. Mechanical characteristics of the structures demonstrating the force applied at the tip of a post needed to bend the post to a given deflection, Y_{lz} = 0.5 μm as a function of A) post bending modulus [l = 8 μm, r = 125 nm]; B) post length [r = 125 nm, and E = 1 GPa]; and C) post radius [l = 8 μm, E = 1 GPa].

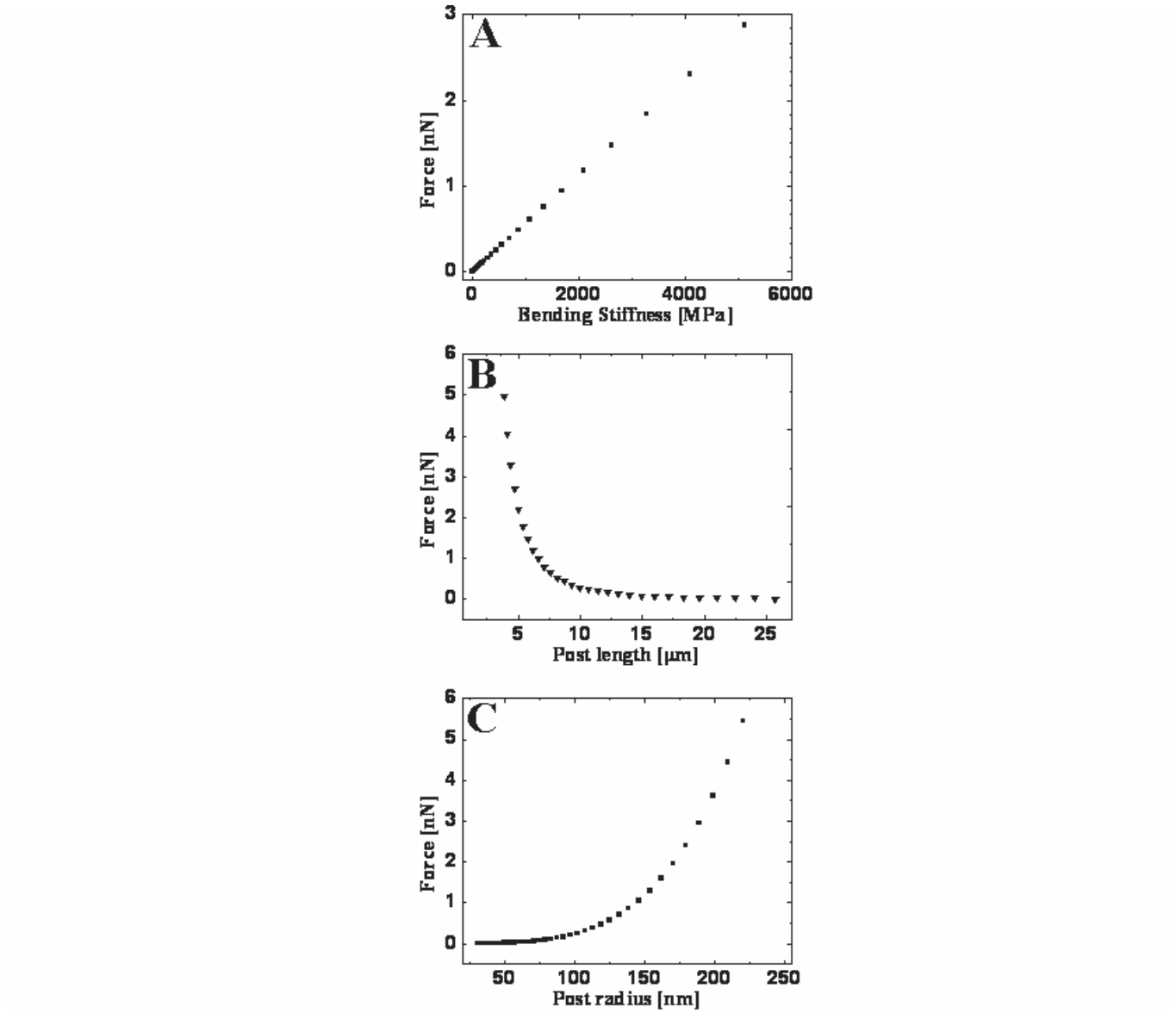

Figure 6. SEM images of the e-beam-actuated epoxy nanoposts. A) Area of posts that have been forced to bend into the center of the e-beam scanning area. This image was captured after focusing at high magnification for a short period and then rapidly increasing the scanning area. The viewing angle is oblique to the surface. B) Illustration of the reversible character of the actuation process, showing snapshots from the full movie (Movie 1 in the supporting online information). From left to right: time zero just as the e-beam was applied; bent posts after the e-beam was focused on the outlined area for 29.5 sec, contrasted with their original condition in the frozen background; extensive post relaxation after the e-beam was allowed to scan a larger area again. C) Illustration of the actuation of the posts that were initially in a tilted position (produced by shearing of the PDMS mold during the epoxy-curing procedure), showing snapshots from the full movie (Movie 2 in the supporting online information). From left to right: time zero just as the e-beam was applied; after 1.2 sec of exposure; after 2.4 sec of exposure; and after 5.3 sec of exposure.

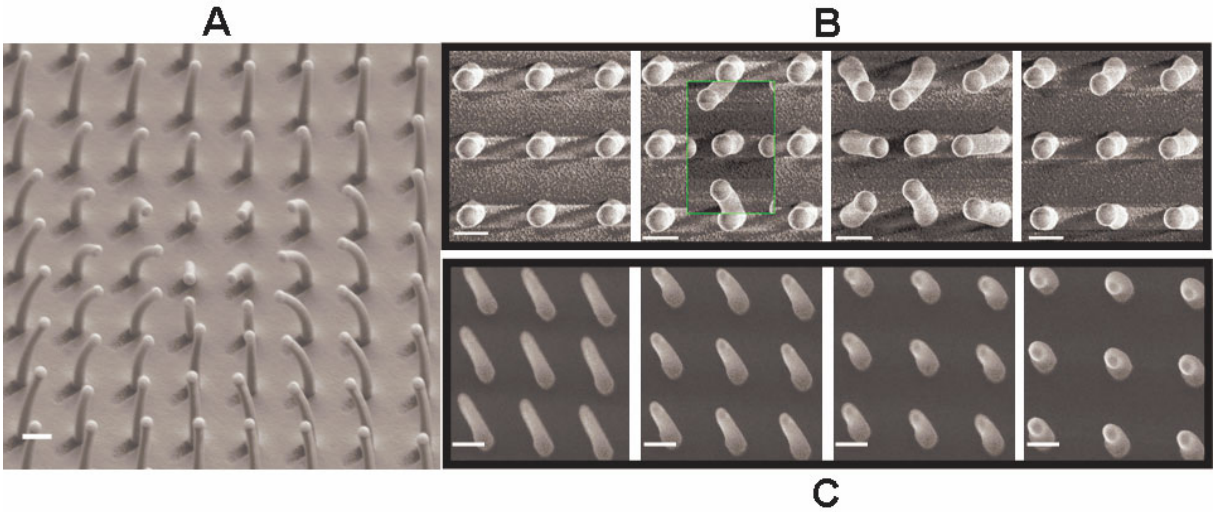

Table 1. Deformation-induced changes in the geometry of the replicated nanostructures [a]

Parameter	**Deformation Type**				
	No deformation	Stretching / compressing along [100]	Stretching / compressing [110]	Shearing along [100]	Compression along [001]
a	a_0	$1/3a_0 < a < 3a_0$	$a_0 < a < 2.1\ a_0$	$a = a_0$	$a \cong a_0$
b	$b_0 = a_0$	$3a_0 > b > 1/3a_0$	$b = a$	$b = a_0$	$b = a$
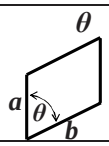	$\theta_0 = 90°$	$\theta = \theta_0$	$12.5° < \theta < 167.5°$	$\theta = \theta_0$	$\theta = \theta_0$
Tilt (*t*) 	$t_0 = 0$	$t = t_0$	$t = t_0$	$0 < t < 63.4°$	$t = t_0$
Post lengths (*l*)	l_0	$l \cong l_0$	$l \cong l_0$	$l_0 < l \leq \sqrt{5}l_0$	$1/3l_0 < l < l_0$
Cross section 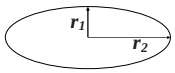	$r_1 = r_2 = r_0$	$r_1 < r_2$	$r_1 < r_2$	$r_1 = r_2 = r_0$	$r_1 = r_2 > r_0$
2D array symmetry	square 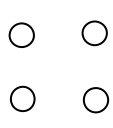	rectangular 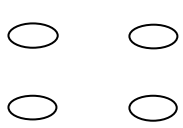	rhombic 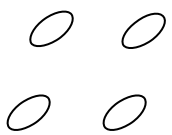	square 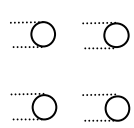	square 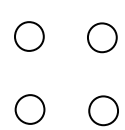

[a] The calculations were made using the reported PDMS extendibility parameter of 300% and Poisson's ratio $\upsilon = 0.5$.[32]

Submitted to ADVANCED MATERIALS

Bio-inspired, multifunctional, high-aspect-ratio nanostructured surfaces are fabricated in a variety of materials with controlled geometry and stiffness. The actuation of the posts is demonstrated.

Keyword: Actuators

B. Pokroy, A. K Epstein, M. C. M. Gulda Person, J. Aizenberg*

Fabrication of Bio-Inspired Actuated Nanostructures with Arbitrary Geometry and Stiffness

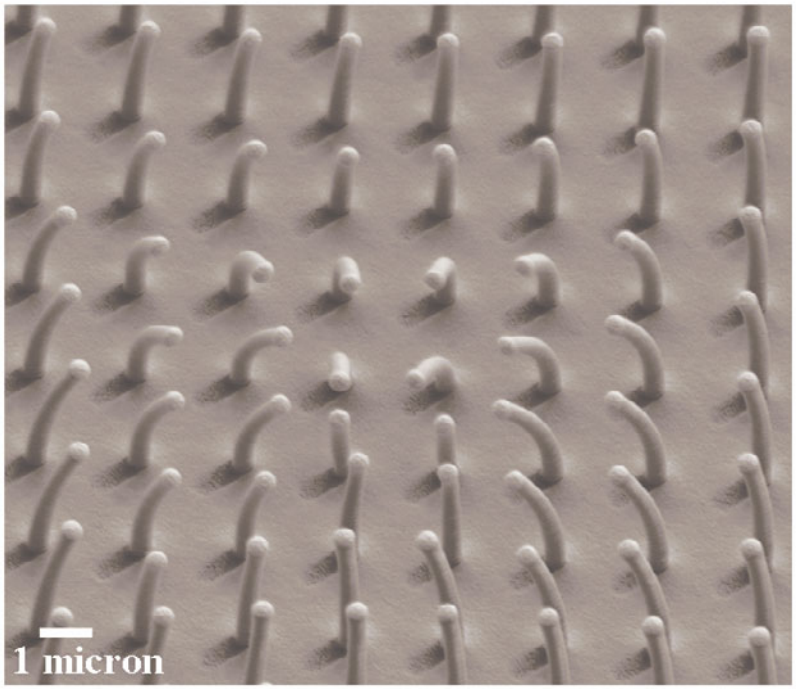

The movies are in the MOV format and can be viewed using the QuickTime® program that can be downloaded from: http://www.apple.com/quicktime/download/

Movie 1: Actuation of the high-aspect-ratio epoxy nanostructures under the e-beam in the SEM. The actuation is reversible and the movie captures multiple actuation cycles. One observes an area of posts that have been forced to bend by the e-beam into the center of the scanning area. This movie was captured after focusing at high magnification for a short period and then rapidly increasing the scanning area. The viewing angle is oblique to the surface. The speed of the video is x5 that of the original.

Movie 2: Actuation of the array of tilted nanostructures under the e-beam in the SEM. The viewing angle is normal to the surface. The speed of the video is x0.4 that of the original.